Statisticalmechanical theory of a new analytical equation of state

Yuhua Song and E. A. Mason

Citation: J. Chem. Phys. **91**, 7840 (1989); doi: 10.1063/1.457252
View online: http://dx.doi.org/10.1063/1.457252
View Table of Contents: http://jcp.aip.org/resource/1/JCPSA6/v91/i12
Published by the American Institute of Physics.

Statistical-mechanical theory of a new analytical equation of state

Yuhua Song and E. A. Mason
Brown University, Providence, Rhode Island 02912

(Received 13 July 1989; accepted 8 September 1989)

We present an analytical equation of state based on statistical-mechanical perturbation theory for hard spheres, using the Weeks–Chandler–Andersen decomposition of the potential and the Carnahan–Starling formula for the pair distribution function at contact, $g(d^+)$, but with a different algorithm for calculating the effective hard-sphere diameter. The second virial coefficient is calculated exactly. Two temperature-dependent quantities in addition to the second virial coefficient arise, an effective hard-sphere diameter or van der Waals covolume, and a scaling factor for $g(d^+)$. Both can be calculated by simple quadrature from the intermolecular potential. If the potential is not known, they can be determined from the experimental second virial coefficient because they are insensitive to the shape of the potential. Two scaling constants suffice for this purpose, the Boyle temperature and the Boyle volume. These could also be determined from analysis of a number of properties other than the second virial coefficient. Thus the second virial coefficient serves to predict the entire equation of state in terms of two scaling parameters, and hence a number of other thermodynamic properties including the Helmholtz free energy, the internal energy, the vapor pressure curve and the orthobaric liquid and vapor densities, and the Joule–Thomson inversion curve, among others. Since it is effectively a two-parameter equation, the equation of state implies a principle of corresponding states. Agreement with computer-simulated results for a Lennard-Jones (12,6) fluid, and with experimental p–v–T data on the noble gases (except He) is quite good, extending up to the limit of available data, which is ten times the critical density for the (12,6) fluid and about three times the critical density for the noble gases. As expected for a mean-field theory, the prediction of the critical constants is only fair, and of the critical exponents is incorrect. Limited testing on the polyatomic gases CH_4, N_2, and CO_2 suggests that the results for spherical molecules (CH_4) may be as good as for the noble gases, nearly as good for slightly nonspherical molecules (N_2), but poor at high densities for nonspherical molecules (CO_2). In all cases, however, the results are accurate up to the critical density. Except for the eight-parameter empirical Benedict–Webb–Rubin equation, this appears to be the most accurate analytical equation of state proposed to date.

I. INTRODUCTION

The quest for a simple analytical equation of state for fluids is very old. The first real success was the van der Waals equation,[1] which can be written as

$$\frac{p}{\rho kT} = \frac{1}{1-b\rho} - \frac{a\rho}{kT}, \tag{1}$$

where p is the pressure, $\rho = N/V$ is the number density, kT has the usual meaning, and a and b are constants for a given fluid. As is well known, this equation shows a critical point and also condensation, when combined with the Maxwell equal-area construction. There have been many attempts over the years to produce modifications of the van der Waals equation having a greater accuracy; a few of the better known ones are those of Dieterici,[2] Beattie and Bridgeman,[3] Benedict, Webb, and Rubin,[4] and Redlich and Kwong.[5] Such equations are widely used in engineering applications.[6,7]

The status of the van der Waals equation plus the Maxwell construction was considerably enhanced, at least among theoreticians, when Kac, Uhlenbeck, and Hemmer[8–11] showed in what sense it could be considered an exact result for a model of hard spheres with weak long-range attractive forces. The main defect is the use of the term $(1-b\rho)^{-1}$ to represent the equation of state of nonattracting hard spheres in three dimensions (the term is exact in one dimension). The term $a\rho/kT$ for the attractive contribution is exact for the model. This accounts for the great improvement in accuracy for real fluids that Haar and Shenker[12] obtained by replacing the term $(1-b\rho)^{-1}$ by a more accurate Percus–Yevick formula, and by using the correct second virial coefficient instead of the van der Waals result of $B_2 = b - a/kT$.

The importance of a hard-sphere model lies in the fact that the structure of simple dense fluids is dominated by the intermolecular repulsive forces.[13] The influence of the attractive forces can then be treated by statistical-mechanical perturbation theory, as can the softness of the repulsions. This approach is very much in the spirit of van der Waals, but the results are far superior, as shown by the pioneering work of Barker and Henderson[14] and of Weeks, Chandler, and Andersen.[15] The subject is now highly developed[16]; given the intermolecular potential, it is possible to predict the thermodynamic properties of simple liquids over their stable range of temperature and density. Unfortunately, considerable numerical computation is required, the effective hard-sphere diameter that appears is a function of both temperature and density, and no simple analytical equation of state is forthcoming.

 0021-9606/89/247840-14$02.10

In this paper we present a simple analytical equation of state, based on statistical-mechanical perturbation theory for a hard-sphere fluid. It is accurate up to about three times the critical density, including the liquid phase, for noble gases, but the accuracy deteriorates for nonspherical molecules at high densities. Even so, for a molecule as nonspherical as CO_2, it is accurate up to the critical density. For a computer-simulated Lennard-Jones fluid, the equation is accurate to about ten times the critical density.

A knowledge of the intermolecular potential allows the complete specification of this equation of state. Three integrations are needed, one to find the second virial coefficient, one to find an effective hard-sphere diameter, and one to find a scaling factor, all as functions of temperature alone. However, the equation is usable with much less input than the full intermolecular potential, since the effective diameter and the scaling factor are nearly universal functions when expressed in suitable reduced units (i.e., they are virtually independent of the detailed *shape* of the potential). The result is that knowledge of the second virial coefficient as a function of temperature enables one to predict the entire equation of state, including the compressibility of the liquid, the vapor-pressure curve, and the critical constants, among other things. It is thus, in effect, a two-parameter equation of state. The results are only moderately accurate in the critical region, presumably because the theory includes a mean-field approximation, and in the low-temperature liquid region, where the Weeks–Chandler–Andersen theory is more accurate.

II. STATISTICAL-MECHANICAL DERIVATION

Our present derivation is similar to that of Weeks, Chandler, and Andersen (WCA),[15] including the division of the intermolecular potential at its minimum into regions of attractive and repulsive force, but differs in two significant respects. The first is that we treat the second virial coefficient exactly rather than by a perturbation method, in order to obtain a good description of the fluid at low densities. The second is our choice of an algorithm for calculating the effective hard-sphere diameter as a function of temperature (only).

We begin with the equation relating pressure to the pair distribution function $g(r)$,[17]

$$\frac{p}{\rho kT} = 1 - \frac{2\pi}{3}\frac{\rho}{kT}\int_0^\infty \frac{du}{dr} g(r) r^3\, dr, \tag{2}$$

where $u(r)$ is the intermolecular pair potential. Underlying this equation are the assumptions that the intermolecular potential is pairwise additive and that the pair potential is central. We next split out the exact second virial coefficient B_2 and rewrite the remainder of the integral in terms of the cavity distribution function $y(r)$,

$$\frac{p}{\rho kT} = 1 + B_2\rho + \rho I, \tag{3}$$

where

$$B_2 = -\frac{2\pi}{3}\beta\int_0^\infty \frac{du}{dr} e^{-\beta u} r^3\, dr$$

$$= 2\pi\int_0^\infty (1 - e^{-\beta u}) r^2\, dr, \tag{4}$$

$$I = \frac{2\pi}{3}\int_0^\infty f(r)[y(r) - 1] r^3\, dr, \tag{5}$$

$$y(r) = e^{\beta u} g(r), \tag{6}$$

$$f(r) = -\beta\frac{du}{dr} e^{-\beta u}, \tag{7}$$

in which $\beta = 1/kT$. The reason for this arrangement of the integral I is that $y(r)$ is smoothly decreasing, and $f(r)$ is sharply peaked, in the repulsive region of the potential. We evaluate I by perturbation theory, using the WCA division of $u(r)$ in which the repulsive forces constitute the unperturbed part. That is, we expect I to be dominated by the repulsion.

The reasons for this expectation are as follows. At high densities (above about the critical density, say), the pressure of a liquid or a highly compressed gas is usually large, and the integral must therefore also be large and positive. The main contribution to the integral thus must come from the repulsion. This is just a reflection of the fact, already mentioned, that the structure of a dense fluid is dominated by the repulsive forces. At lower densities we can think about a virial expansion of the integral, which starts with the third virial coefficient. The third, fourth, and fifth virial coefficients are all positive or small above the critical temperature,[18] so that the integral is positive and again dominated by the repulsion. Below the critical temperature the density of even the saturated vapor is so low that its behavior is largely described by just B_2, and the integral is virtually negligible.

To evaluate I we therefore pick the unperturbed potential u_0 to be

$$u_0(r) = \begin{cases} u(r) + \epsilon, & r < r_m \\ 0, & r > r_m \end{cases}, \tag{8}$$

where ϵ is the depth of the potential well and r_m is its minimum position. The part of the function $f(r)$ in the integrand of I that corresponds to u_0 then becomes

$$f_0(r) = \begin{cases} -\beta\dfrac{du_0}{dr} e^{-\beta u_0}, & r < r_m \\ 0, & r > r_m \end{cases}. \tag{9}$$

The functions $y(r)$ and $f_0(r)$ are shown in Fig. 1 for a Lennard-Jones (12,6) potential.[19] The oscillations in $y(r)$ for $r > r_m$ allow us to set the upper limit of I equal to r_m rather than infinity. Moreover, we can replace $y(r)$ by $y_0(r)$ in the integrand, because the two are quite similar.[19] Making these approximations, and expanding $f(r) = f_0(r)(1 + \beta\epsilon + \cdots)$, we obtain

$$I \approx \frac{2\pi}{3}\int_0^{r_m} f_0(r)(1 + \beta\epsilon)[y_0(r) - 1] r^3\, dr. \tag{10}$$

The rather sharp peak in $f_0(r)$ at some position $r_0(T) < r_m$ makes it possible to evaluate this integral by noting that the dominant contribution to I comes from the neighborhood of r_0, where $y_0(r)$ behaves to first order as a straight line,

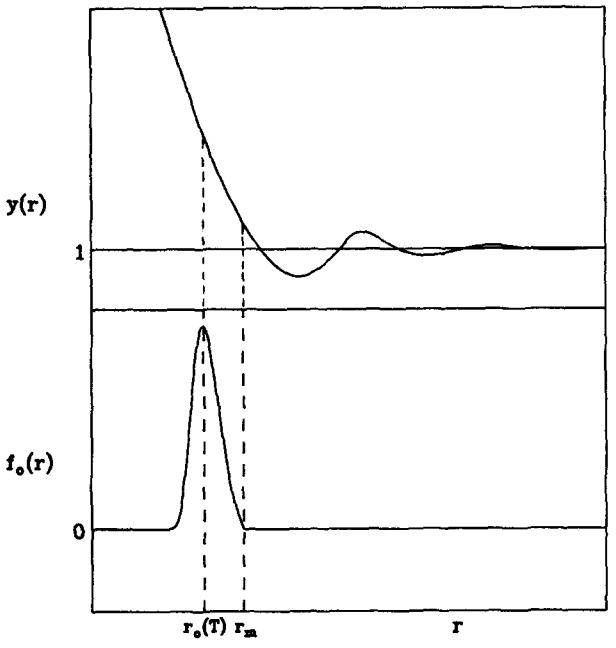

FIG. 1. The cavity distribution function $y(r)$ and the weighting function $f_0(r)$ of Eq. (9), illustrated for a (12,6) potential.

$$y_0(r) = y_0(R) + \left(\frac{dy_0}{dr}\right)_R (r - R) + \cdots, \tag{11}$$

where R is a point near r_0, left unspecified for the moment. Then I becomes

$$I \approx I_0 + I_+ + I_- + \cdots, \tag{12}$$

where

$$I_0 = \frac{2\pi}{3}[y_0(R) - 1]\int_0^{r_m} f_0(r) r^3\, dr, \tag{12a}$$

$$I_+ = \frac{2\pi}{3}\beta\epsilon[y_0(R) - 1]\int_0^{r_m} f_0(r) r^3\, dr, \tag{12b}$$

$$I_- = \frac{2\pi}{3}[y_0(R) - 1]\left(\frac{dy_0}{dr}\right)_R \int_0^{r_m} f_0(r)(r - R) r^3\, dr. \tag{12c}$$

For any reasonable choice of R, the integrals I_+ and I_- are positive and negative, respectively, at all temperatures. At middle to high temperatures they are usually negligible compared to I_0. At low temperatures they are not individually negligible, but tend to cancel. It is thus a reasonable approximation to write

$$I \approx I_0 = \alpha[y_0(R) - 1], \tag{13}$$

$$\alpha(T) = \frac{2\pi}{3}\int_0^{r_m} f_0(r) r^3\, dr = 2\pi\int_0^{r_m} (1 - e^{-\beta u_0}) r^2\, dr. \tag{14}$$

Since $y_0(r)$ is fairly insensitive to the form of the potential, and in fact is rather accurately mimicked by a hard-sphere model,[19] we replace $y_0(R)$ by the corresponding function $y_d(d)$ for hard spheres of diameter d,

$$y_0(R) \approx y_d(d) = g(d^+), \tag{15}$$

where $g(d^+)$ is the pair distribution function of hard spheres at contact. Presumably d is fairly close to R, but this detail is irrelevant for our purposes.

Substituting all these results back into Eq. (3), we obtain an equation of state of the form

$$\frac{p}{\rho kT} = 1 + B_2\rho + \alpha\rho[g(d^+) - 1], \tag{16}$$

which contains three temperature-dependent parameters, $B_2(T)$, $\alpha(T)$, and $d(T)$. The first two are given explicitly in terms of the intermolecular potential by Eqs. (4) and (14). All that can be said about $d(T)$ at this point is that it must lie between 0 and r_m.

The structure of Eq. (16) is interesting. It consists of an ideal-gas term plus an exact second virial coefficient, and the rest of the equation of state is then represented by an equivalent hard-sphere expression multiplied by a temperature-dependent scaling factor $\alpha(T)$. Because of our treatment of $y(r)$ it is obviously a mean-field theory, and in fact it has a close resemblance to the van der Waals equation. This can be seen by rewriting Eq. (1) as

$$\frac{p}{\rho kT} = 1 + \left(b - \frac{a}{kT}\right)\rho + b\rho\left(\frac{1}{1 - b\rho} - 1\right). \tag{17}$$

Thus our Eq. (16) reduces to the van der Waals equation if we treat B_2 by first-order perturbation theory, evaluate α for hard spheres from Eq. (14), giving $\alpha = 2\pi d^3/3 = b$, and approximate $g(d^+)$ crudely[20] as $(1 - b\rho)^{-1}$.

To obtain an explicit equation of state from Eq. (16), we must pick a suitable mathematical form for $g(d^+)$ and an algorithm for determining $d(T)$. The latter we defer to the next section; the former we can do immediately. The Carnahan–Starling[21] expression for $g(d^+)$ is remarkably accurate:

$$g(d^+) = \frac{1 - \frac{1}{2}\eta}{(1 - \eta)^3}, \tag{18}$$

where η is the packing fraction,

$$\eta = \frac{\pi}{6} d^3\rho = \frac{1}{4} b\rho. \tag{19}$$

This formula is accurate up to the freezing density. More complicated formulas that are accurate for the higher densities of the metastable fluid are available,[22,23] but are not needed here. With this choice of $g(d^+)$, the equation of state is quintic in the volume, in contrast to the cubic van der Waals equation and the quartic Beattie–Bridgeman equation.

III. CHOICE OF EFFECTIVE HARD-SPHERE DIAMETER

It is convenient to discuss the effective hard-sphere diameter in terms of the corresponding effective van der Waals covolume b,

$$b \equiv \tfrac{2}{3}\pi d^3. \tag{20}$$

The foregoing statistical-mechanical arguments do not give a definite prescription for the calculation of b, as they do for $B_2(T)$ and $\alpha(T)$, but they do suggest limiting behaviors at low and high temperatures, from which a suitable algorithm for the calculation of $b(T)$ can be devised.

According to the WCA decomposition of $u(r)$, the maximum value of d will be r_m in the limit of $T \to 0$, so that

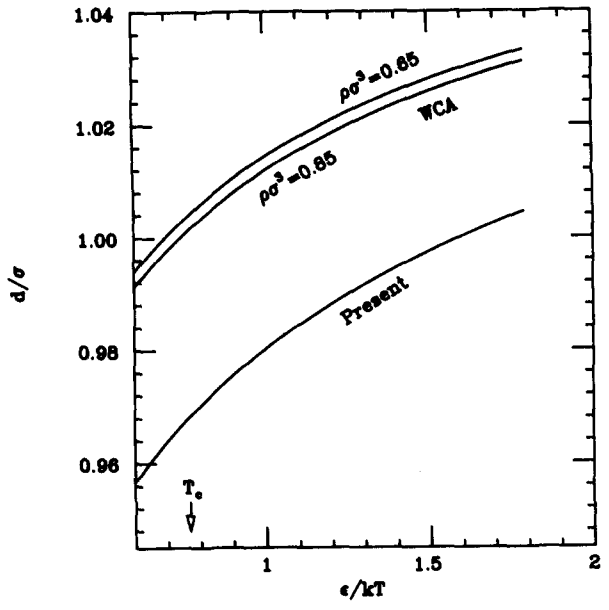

FIG. 2. Effective hard-sphere diameters according to the WCA theory for dense fluids, compared to the present theory, for the (12,6) potential.

$$b(T\to 0) = \tfrac{2}{3}\pi r_m^3. \tag{21}$$

This takes care of the low-temperature limit.

At high temperatures, say in the vicinity of the Boyle temperature (where $B_2 = 0$), the behavior of B_2 can be represented rather well by the van der Waals formula

$$B_2(T) = b - \frac{a}{kT}. \tag{22}$$

From this we obtain, by ignoring any temperature dependence of b and a, a high-temperature limiting form for b:

$$b(T\to\text{high}) = B_2 + T\frac{dB_2}{dT} = 2\pi\int_0^\infty [1-(1+\beta u)e^{-\beta u}]r^2\,dr. \tag{23}$$

However, this expression is not suitable at low temperatures because it leads to $b(T\to 0)\to\infty$.

A simple formula for b that behaves properly at all temperatures can be obtained from the above results by thinking of b as the excluded volume due to the repulsive forces only; then Eq. (23) becomes

$$b(T) = 2\pi\int_0^{r_m} [1-(1+\beta u_0)e^{-\beta u_0}]r^2\,dr. \tag{24}$$

This gives the correct limiting behavior at both high and low temperatures, and behaves smoothly in between. Moreover, it gives a relationship between $b(T)$ and $\alpha(T)$:

$$b = \alpha + T\frac{d\alpha}{dT}, \tag{25}$$

which is valid at all temperatures. This completes the specification of the equation of state.

The algorithm of Eq. (24) for $b(T)$ or $d(T)$ may be compared with that of WCA, who obtained d by equating the compressibility of the reference system having a potential u_0 to that of a hard-sphere system. Because the compressibility depends on ρ as well as on T, the resulting value of d also depends on both ρ and T, whereas the value of d from Eq. (24) depends only on T. The results are compared in Fig. 2 for a (12,6) potential. The present value of d is lower by about 4% than the calculation of WCA in the range shown (which corresponds to a fluid of about 3 times critical density), but the variation with temperature is quite similar.

IV. EQUATION OF STATE

The final result for the equation of state, explicit in the density, is

$$\frac{p}{\rho kT} = 1 + B_2\rho + \alpha\rho\left[\frac{8(8-b\rho)}{(4-b\rho)^3} - 1\right], \tag{26}$$

with $B_2(T)$, $\alpha(T)$, and $b(T)$ given in terms of the intermolecular potential by Eqs. (4), (14), and (24), respectively:

$$B_2(T) = 2\pi\int_0^\infty (1-e^{-\beta u})r^2\,dr, \tag{4}$$

$$\alpha(T) = 2\pi\int_0^{r_m} (1-e^{-\beta u_0})r^2\,dr, \tag{14}$$

$$b(T) = 2\pi\int_0^{r_m} [1-(1+\beta u_0)e^{-\beta u_0}]r^2\,dr = \alpha + T\frac{d\alpha}{dT}. \tag{24}$$

From these equations we notice the following additional relation:

$$\alpha(T\to\text{high}) = B_2. \tag{27}$$

For hard spheres we have $b = \alpha = B_2$, and we recover the Carnahan–Starling[21] equation of state.

A. The parameters $\alpha(T)$ and $b(T)$

In practice, the potential $u(r)$ is seldom accurately known, although B_2 itself can be found experimentally. In such cases Eq. (24) can be regarded as an equation of state with two unknown temperature-dependent parameters, α and b, or one temperature-dependent parameter if the relation in Eq. (25) is invoked. The temperature dependence of α and b argues against treating them simply as adjustable parameters, because the results would be mostly curve fitting with little predictive power. However, it turns out that α and b are rather insensitive to the *shape* of $u(r)$, although of course not to its scale, so that they appear as almost universal functions of temperature in terms of suitable reduced units.

Suitable reduced units can be chosen by imagining that $B_2(T)$ is known, and that the parameters ϵ and r_m for some model potential $u(r)$ are found by fitting B_2, preferably in the region of the Boyle temperature. The values of ϵ and r_m will depend on the particular model chosen, but they will always be such as to reproduce the values of the Boyle temperature T_B, the Boyle volume v_B, and the Boyle pressure p_B, defined as

$$B_2(T_B) = 0, \quad v_B \equiv T_B\left(\frac{dB_2}{dT}\right)_{T_B}, \quad p_B \equiv \frac{kT_B}{v_B}. \tag{28}$$

That is, reduced quantities such as kT_B/ϵ and v_B/r_m^3 will be model dependent, but T_B and v_B themselves are fixed experimental quantities. The reduced quantities α/v_B and b/v_B as

functions of T/T_B should then be nearly the same for different models of $u(r)$, the peculiarities of the models having been suppressed by fitting the same data on B_2.

This behavior is shown in Fig. 3, where results for a Lennard-Jones (12,6) potential and for an accurate potential for argon devised by Aziz and Chen[24] are shown. Also shown for comparison is B_2/v_B. The values of α/v_B and b/v_B are rather insensitive to the potential, and for most practical purposes can be considered to be essentially universal functions of T/T_B.

The significance of this result is that knowledge of just $B_2(T)$ is sufficient to determine both $\alpha(T)$ and $b(T)$ with reasonable accuracy, from which the entire equation of state, including the liquid branches, can be predicted. For this purpose we give in Table I values of α/v_B, b/v_B, and B_2/v_B as functions of T/T_B. Although the numbers were calculated for a (12,6) potential, Fig. 3 shows that they are almost universal. If it is inconvenient to find T_B and v_B directly from experimental data, the values of ϵ and r_m for some reasonable model can be found by fitting whatever data are available, and then T_B and v_B calculated from these. For this purpose values of kT_B/ϵ and v_B/σ^3 for several models of $u(r)$ are given in Table II. Here σ is the value of r such that $u(\sigma) = 0$.

The significance of this near universality of the temperature-dependent parameters is that the present equation of state must follow a two-parameter (ϵ, r_m or σ) correlation, or principle of corresponding states.

TABLE I. Reduced values of the temperature-dependent parameters α, b, and B_2.

T/T_B	α/v_B	b/v_B	B_2/v_B
0	1.7433	1.7433	$-\infty$
0.1	1.4313	1.3200	−24.4935
0.2	1.3481	1.2197	−6.0531
0.3	1.2942	1.1570	−2.9945
0.4	1.2539	1.1113	−1.7752
0.5	1.2217	1.0752	−1.1254
0.6	1.1947	1.0456	−0.7241
0.7	1.1716	1.0204	−0.4531
0.8	1.1513	0.9986	−0.2586
0.9	1.1332	0.9794	−0.1128
1	1.1170	0.9622	0.0000
2	1.0083	0.8505	0.4544
3	0.9444	0.7872	0.5735
4	0.8994	0.7437	0.6196
5	0.8648	0.7108	0.6398
6	0.8369	0.6845	0.6485
7	0.8135	0.6628	0.6513
8	0.7935	0.6444	0.6511
9	0.7760	0.6284	0.6490
10	0.7605	0.6143	0.6458
20	0.6628	0.5274	0.6042
30	0.6093	0.4811	0.5698
40	0.5732	0.4503	0.5433
50	0.5462	0.4276	0.5222
60	0.5249	0.4097	0.5048
70	0.5074	0.3952	0.4901
80	0.4926	0.3829	0.4774
90	0.4798	0.3724	0.4662
100	0.4686	0.3632	0.4563
∞	0	0	0

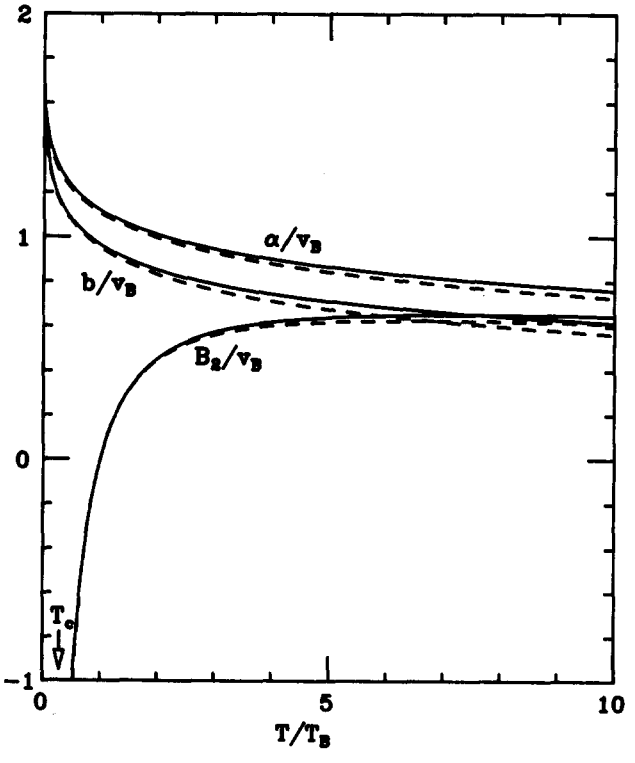

FIG. 3. Reduced plots of the parameters $\alpha(T)$ and $b(T)$ for different potential models, showing the nearly universal behavior in terms of the Boyle parameters. The second virial coefficient $B_2(T)$ is also shown for comparison. The solid curves are for the (12,6) potential and the dashed curves for the Aziz–Chen argon potential.

Because of the near universality of $\alpha(T)$, $b(T)$, and $B_2(T)$ when expressed in a suitable reduced form, most of our subsequent calculations use a (12,6) potential for convenience.

B. Critical constants and exponents

Once B_2, α, and b are known, it is straightforward to calculate the critical constants of the present equation of state from the usual conditions on derivatives of the critical p–v isotherm. The results are shown in Table III as calculated for the (12,6) potential and for the Aziz–Chen argon potential. As expected, these results are very close in terms of the Boyle parameters, the greatest difference being 4% in the critical pressures. For comparison, the (not very accurate) molecular dynamics[25(a)] and cluster-integral[25(b)] calculations for the (12,6) potential and the experimental results[26] for argon are also shown. The agreement is only fair. However, the agreement between the molecular dynamics results

TABLE II. Values of Boyle parameters for several potential models, including $p_B\sigma^3/\epsilon = (kT_B/\epsilon)(\sigma^3/v_B)$.

Potential	kT_B/ϵ	v_B/σ^3	$p_B\sigma^3/\epsilon$
9,6	4.555	1.498	3.041
12,6	3.418	1.699	2.012
Aziz–Chen	2.856	1.750	1.632

TABLE III. Calculated and experimental critical constants.

	T_c/T_B	ρ_c/ρ_B	p_c/p_B	$Z_c = p_c/\rho_c kT_c$
Present				
(12,6)	0.382	0.446	0.0609	0.357
Aziz–Chen	0.392	0.452	0.0634	0.358
(12,6)				
Molecular dynamics	0.39–0.40	0.54–0.61	0.065–0.085	0.30–0.36
Cluster integrals	0.374	0.455	0.0570	0.34
Argon	0.369	0.535	0.0586	0.297
van der Waals	0.296	0.333	0.0370	0.375

and the argon data is also only fair. This may be due in part to many-body forces, which were not included in the molecular dynamics but which doubtless occur in argon in the critical region.

The corresponding predictions of the critical constants for the van der Waals potential are also shown in Table III, using Boyle parameters calculated from the van der Waals expression for B_2 of Eq. (22), namely $b = v_B$ and $a = kT_B v_B$. The critical constants are all much too low, although their combination into the critical compressibility factor Z_c turns out to be too large.

Since the present equation of state is based on a mean-field theory, we do not expect it to be very accurate in the critical region, although the results in Table III are not bad for an analytical equation of state. The discrepancies show up more clearly in the critical exponents.[27] The present equation yields the "classical," or van der Waals, exponents expected of a mean-field theory. For instance, the exponent β that describes the shape of the upper part of the two-phase region is predicted to be 1/2, instead of the correct value of $\beta \approx 0.33$. In its defense, however, we can claim for the present theory that no other analytical equation of state gives correct critical exponents, either.

C. p–T isochores (isometrics)

Even the earliest investigators of fluid compressibility were impressed by the fact that the curves of constant density in a p–T plot (isochores or isometrics) were nearly linear for real fluids,[28] although very different from the linear perfect-gas isochores. Any sensible equation of state must thus give nearly linear isochores. On closer inspection, the isochores of real fluids show small negative curvatures (concave downwards) at both low and high densities. The general experimental situation is less clear at intermediate densities, but at least a number of the lower hydrocarbons show a region of small positive curvature.[29]

The isochores of the van der Waals equation are all linear, those of the Dieterici equation all show positive curvature, and those of the Beattie–Bridgeman and Redlich–Kwong equations all show negative curvature. Only the eight-parameter equation of Benedict, Webb, and Rubin manages to shift from negative to positive and back to negative curvature as the density increases.

Our results for the (12,6) potential are shown in Fig. 4, as p/p_c vs T/T_c at a number of constant values of ρ/ρ_c. The isosochores all show a small negative curvature, and are thus consistent with the behavior of most gases, insofar as it is known.

D. Virial coefficients

Expansion of Eq. (26) gives an infinite series in the density

$$\frac{p}{\rho kT} = 1 + B_2\rho + \alpha\rho\left[\tfrac{5}{8}(b\rho) + \tfrac{9}{32}(b\rho)^2 + \tfrac{7}{64}(b\rho)^3 + \cdots\right], \tag{29}$$

from which the higher virial coefficients are identified as

$$B_3(T) = \tfrac{5}{8}\alpha b,$$
$$B_4(T) = \tfrac{9}{32}\alpha b^2, \tag{30}$$
$$B_5(T) = \tfrac{7}{64}\alpha b^3, \text{ etc.}$$

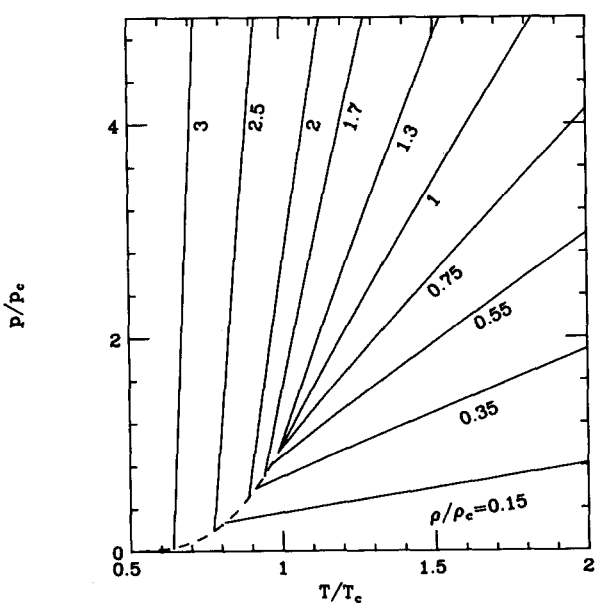

FIG. 4. Reduced isochores (isometrics) of the present equation of state as calculated for the (12,6) potential. The numbers on the isochores are the values of ρ/ρ_c. The dashed portion is the vapor-pressure curve, terminating at the critical point.

The numerical factors are just the Carnahan–Starling values for the hard-sphere virial coefficients. Referring to Fig. 3 for the temperature dependence of α and b, we see that the higher virial coefficients of the present theory must be monotonically decreasing functions of T. This is obviously incorrect at very low temperatures, where higher virial coefficients must become negative because of cluster formation.[30] It turns out that this discrepancy is unimportant because of the low temperatures at which it occurs, as discussed below.

Third, fourth, and fifth virial coefficients from the present equation of state are compared with exact calculations[31] for the (12,6) potential in Fig. 5. The present results give a fair representation of the true virial coefficients down to about the critical temperature, but at lower temperatures the exact virial coefficients turn over and eventually become negative, as expected. Thus the present results should be good above the critical temperature. It is interesting to note that in this temperature region it is known empirically that the fourth virial coefficient is sufficient to give the pressure accurately up to nearly the critical density. This is shown by the fact that the Beattie–Bridgeman equation, which is accurate up to about the critical density,[28,29] terminates at the fourth virial coefficient when written in virial form. It has also been noticed empirically that inclusion of just the fourth virial coefficient suffices to fit the critical isotherm itself for pressures below the critical.[32] Since the present equation contains approximations for *all* the virial coefficients, we can anticipate that it should be good at densities even higher than critical when $T > T_c$.

For $T < T_c$, the highest gas density attainable is that of the saturated vapor. This density is usually low enough that the contributions of the higher virial coefficients are unimportant, and the present equation of state thus should still be accurate because it uses the correct second virial coefficient, even though its representation of the higher virial coefficients is incorrect.

Thus the behavior of the virial coefficients suggests that the present equation of state should behave in a reasonable way up to high densities for $T > T_c$, and up to the saturated vapor density for $T < T_c$. The question of the behavior of the high-density liquid ($T < T_c$) is left open, since the virial expansion is inapplicable.

These matters are tested empirically in the next section.

An additional, although fortuitous, benefit of the present equation can be seen in Fig. 5. The experimental points for B_3 lie generally above the calculated exact curve, and this deviation is commonly regarded as caused by three-body forces.[33] Since the present results deviate from the exact curve in the same direction, there may be some compensation of errors when application is made to real fluids.

V. COMPARISON WITH EXPERIMENTAL p–v–T DATA

A vast amount of p–v–T data exists,[18] and we must confine our comparisons to a few selected systems. These consist, first, of the Lennard-Jones (12,6) fluid and the heavier noble gases Ne, Ar, Kr, and Xe. We omit He because of the quantum corrections. The assumptions of the theory should apply rather well to these systems. Second, we consider three polyatomic molecules—spherical CH_4, moderately nonspherical N_2, and distinctly nonspherical CO_2. Finally we consider Hg, which exhibits ordinary closed-shell atomic in-

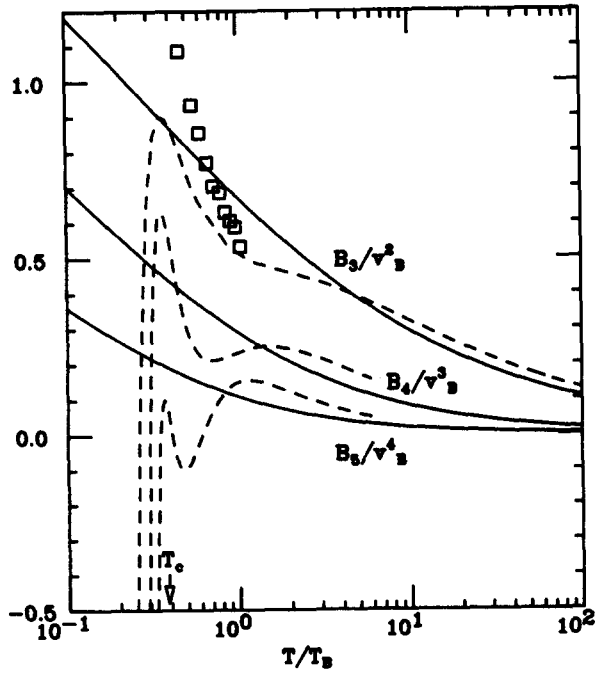

FIG. 5. Higher virial coefficients from the present equation of state (solid curves) compared with exact calculations for the (12,6) potential (dashed curves). The points are experimental values of B_3 for argon.

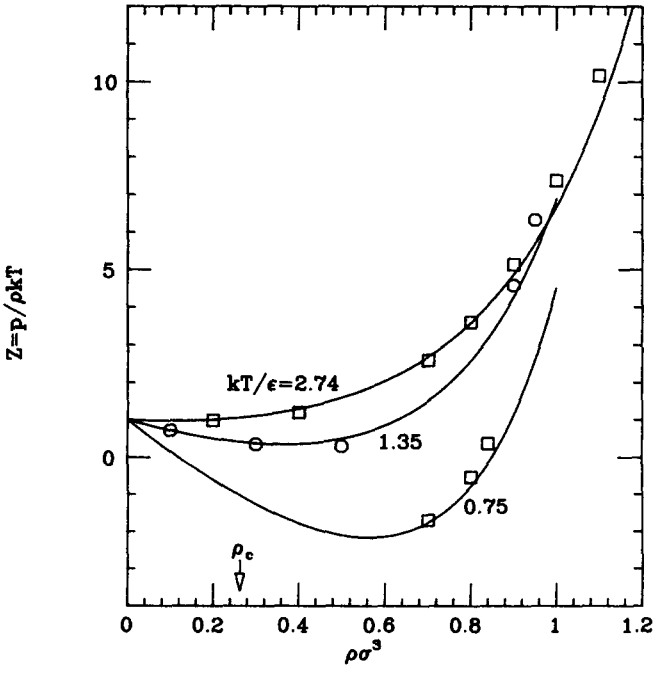

FIG. 6. Compressibility factors as a function of reduced density for a Lennard-Jones (12,6) fluid. The reduced critical temperature is near 1.35. The curves are *a priori* calculations from the potential, and the points are computer simulations.

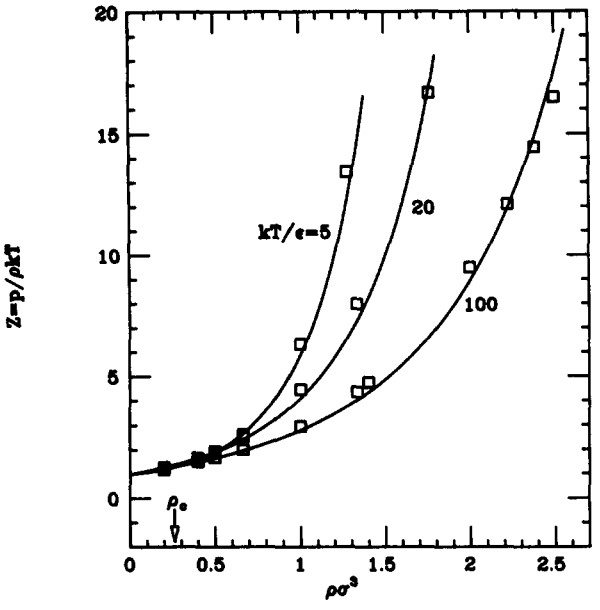

FIG. 7. Same as Fig. 6, but for higher temperatures and densities.

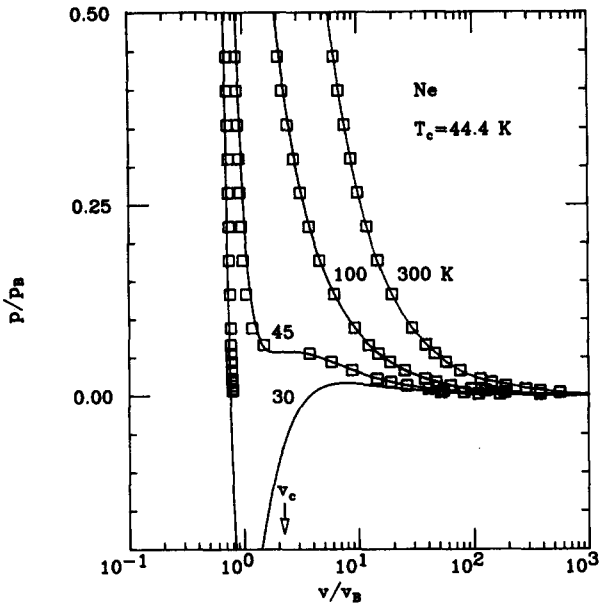

FIG. 8. Reduced p–v isotherms for neon. The curves are calculated from a fit of the experimental second virial coefficient. The points are from Ref. 26.

teractions at low densities, but metallic interactions and free electrons at high densities.

A. Lennard-Jones (12,6) fluid

The results for this mythical fluid are shown in Figs. 6 and 7 as plots of the compressibility factor $Z = p/\rho kT$ vs reduced density $\rho\sigma^3$, for several reduced temperatures kT/ϵ. The curves are completely *a priori* calculations from the potential, according to Eqs. (4), (14), and (24) for $B_2(T)$, $\alpha(T)$, and $b(T)$, respectively. The "experimental data" are from computer simulations and are taken from the summary of Kang *et al.*[34] The agreement is somewhat variable, but is better than 1% at low densities and roughly a few percent at densities well above the critical. Notice that at $kT/\epsilon = 0.75$, two of the points are in the metastable liquid region with negative pressures. Notice also that at $kT/\epsilon = 100$, the agreement extends to about ten times the critical density.

The calculated curves of course do not show the two-phase vapor–liquid region, since Eq. (26) represents an analytic function. A Maxwell equal-area construction must be added. This feature can be seen more clearly in plots of p vs v, shown next for the noble gases.

B. Noble gases

Three or four p/p_B vs v/v_B isotherms are shown for each of the systems Ne, Ar, Kr, and Xe in Figs. 8–11. Here the two-phase region is evident, although we have not explicitly drawn in the Maxwell construction. The curves are calculated from the second virial coefficients, using a (12,6) potential to determine $\alpha(T)$ and $b(T)$. As Fig. 3 shows, the results are insensitive to the particular potential used. For completeness, the relevant potential parameters used are listed in Table IV. They are taken from the summaries given by Hirschfelder, Curtiss, and Bird,[35] but the values for Xe have been adjusted slightly (within experimental uncertainty) to produce a better fit of the liquid branch. The experimental data are mostly from the convenient compilation of Vargaftik,[26] augmented by data from Theeuwes and Bearman[36] (Kr) and from Michels *et al.*[37] (Xe).

The accuracy of the results is rather remarkable, especially considering that they are based essentially on second virial coefficients. Below the critical density the agreement is usually considerably better than 1%, and even in the steep liquid branch the agreement of the calculated and measured densities (at fixed pressure) is within a few percent. Notice

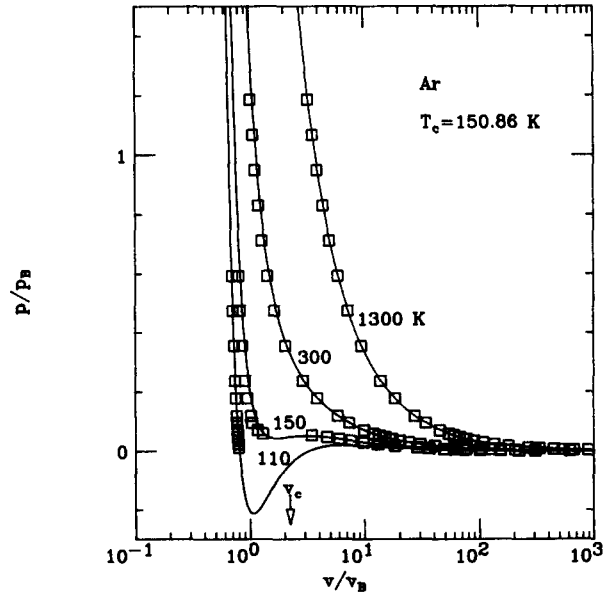

FIG. 9. Same as Fig. 8, for argon.

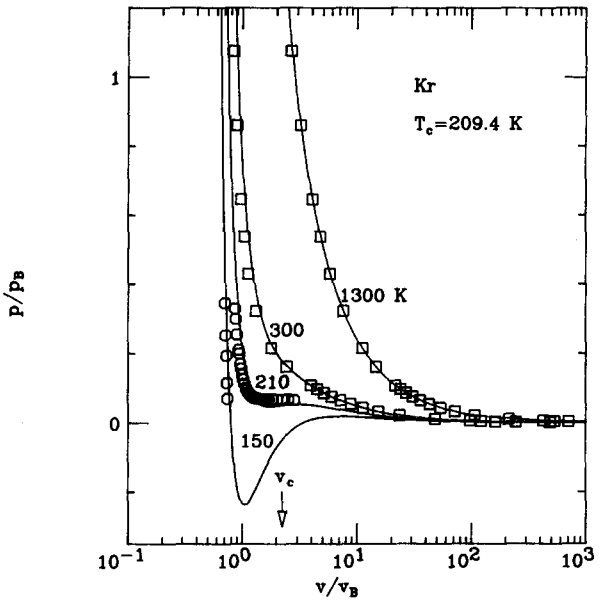

FIG. 10. Same as Fig. 8, for krypton. The squares are from Ref. 26 and the circles from Ref. 36.

that the good agreement extends up to about three times the critical density, which is the limit of the data. Modest adjustments of the potential parameters—within the experimental uncertainty of the second virial coefficients—would improve the agreement even more, but we have not attempted to optimize the fits.

Not too surprisingly, the poorest agreement seems to occur in the vicinity of the critical point, and especially on the high density side of the critical isotherm. Even so, the critical temperatures are predicted fairly well: 3% for Ne, 4% for Ar and Kr, and 6% for Xe (as calculated from Tables II–IV). The predicted critical pressures are also fairly good: 4% for Ne, 3% for Ar and Kr, and 10% for Xe.

TABLE IV. Lennard-Jones (12,6) parameters used in calculating the isotherms of Figs. 8–14.

Gas	ϵ/k(K)	σ(Å)
Ne	34.9	2.78
Ar	119.8	3.405
Kr	166.7	3.679
Xe	234.9	3.955
CH_4	152.1	3.725
N_2	95.05	3.698
CO_2	219.6	3.925

No effects of many-body forces, which are not included in the theory, seem to be evident. As suggested by the higher virial coefficients shown in Fig. 5, there may be some compensation of errors at lower densities, but Figs. 8–11 show that the agreement is still good at liquid densities. It is not obvious whether this is due to the actual unimportance of many-body forces or to some remarkably fortuitous cancellation of errors.

C. Polyatomic gases

Analogous results are shown in Figs. 12–14 for CH_4, N_2, and CO_2. The (12,6) parameters used in the calculations are listed in Table IV, and the experimental data are taken from Vargaftik.[26] We have slightly adjusted the parameters for CH_4 and CO_2 to see whether the liquid densities can be reproduced, but the parameters for N_2 are as given by Hirschfelder *et al.*[35] In any case, the calculated curves can be considered to be predictions based on experimental second virial coefficients.

The agreement shown in Fig. 12 for the spherical molecule CH_4 is as good as that for the noble gases. The predicted critical temperature is in error by 4%, and the critical pressure by 7%.

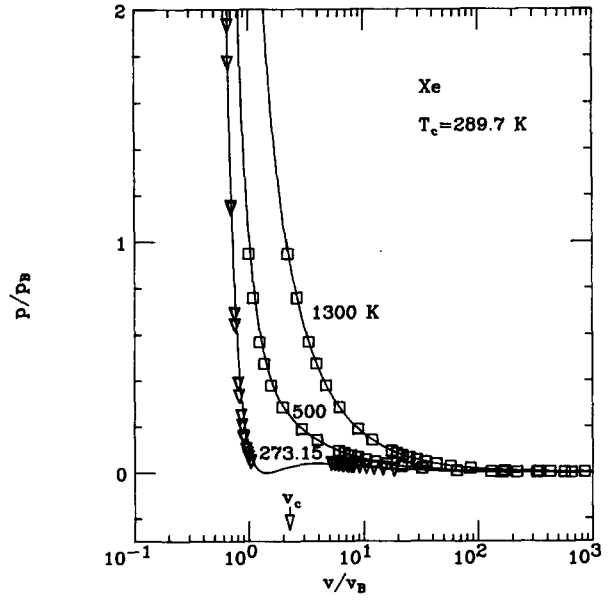

FIG. 11. Same as Fig. 8, for xenon. The squares are from Ref. 26 and the triangles from Ref. 37.

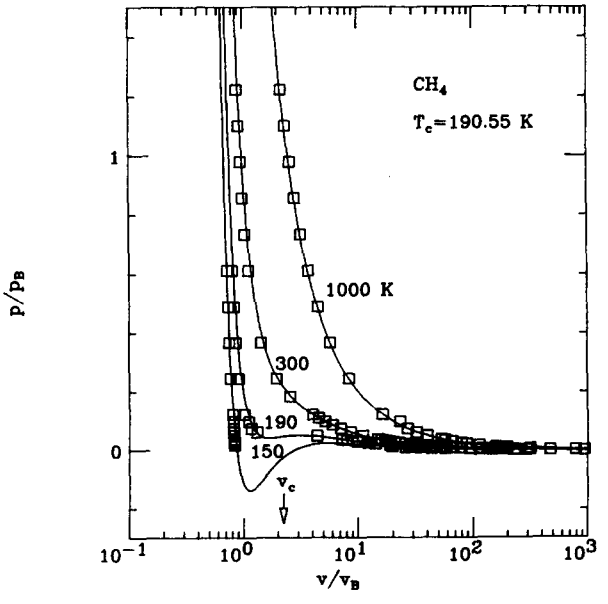

FIG. 12. Same as Fig. 8, for methane.

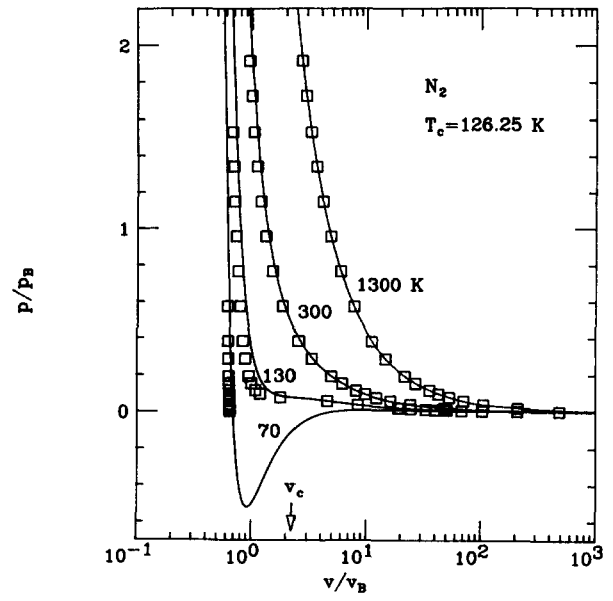

FIG. 13. Same as Fig. 8, for nitrogen.

Some deviations can be seen for N_2 in Fig. 13, especially near the critical isotherm, but the agreement for densities below the critical is as good as for the noble gases. Even the liquid branch at 70 K is not bad. The predicted critical temperature is in error by only 2%, and the critical pressure by 6%. Although the fit could be improved by some moderate adjustment of potential parameters, the suspicion lingers that we are seeing the effects of molecular anisotropy.

The suspicion is reinforced by the results for CO_2, shown in Fig. 14. Here the predicted liquid branch is seriously in error, and no parameter adjustment can save it. Nevertheless, the results for densities less than the critical density are still very good, and the predicted critical temperature is off by only 6%. The critical pressure, however, is off by 17%.

The foregoing results suggest that the present theory can generally use second virial coefficients to predict accurate p–v isotherms below the critical density, but that effects of molecular shape become manifest at higher densities.

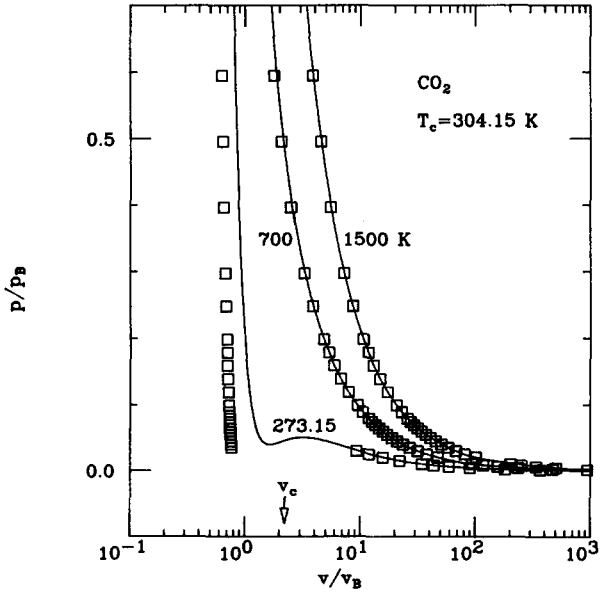

FIG. 14. Same as Fig. 8, for carbon dioxide.

D. Mercury

Viewed as a dilute gas, mercury is farily ordinary,[38] but viewed as an expanded liquid metal it is decidedly peculiar.[39] Its behavior with respect to the present equation of state is also very peculiar, as can be seen by even a cursory analysis. It is not possible to choose a single potential that will describe its p–v–T properties over an extended range, which means that it cannot be described by the present equation of state. An easy way to see this is to predict the critical temperature and pressure from potentials fitted to low-temperature vapor and liquid data.

Epstein and Powers[38] have analyzed the viscosity of mercury vapor in the range 218–610 °C in terms of a (12,6) potential and obtain the parameters

$$\epsilon/k = 851 \pm 32 \text{ K},$$
$$\sigma = 2.89_8 \pm 0.03_9 \text{ Å}. \tag{31}$$

These are consistent with the extremely meager data on the second virial coefficient.[40] From these results and the entries in Tables II and III, we calculate $T_c = 1111$ K and $p_c = 592$ bar, which are very far from the experimental values[41] of 1763 K and 1510 bar.

Moelywn-Hughes[42] has analyzed the properties of liquid mercury in terms of a (9,6) potential and obtained the parameters

$$\epsilon/k = 795 \text{ K},$$
$$\sigma = 2.95 \text{ Å}, \tag{32}$$

which are not in bad agreement with those from the vapor viscosity. These parameters lead, according to the present equation of state, to critical constants of $T_c = 1307$ K and $p_c = 692$ bar, again very far from the experimental values.

The conclusion is that low-temperature p–v isotherms of mercury are completely inconsistent with the higher-temperature isotherms near the critical isotherm, in terms of the present equation of state. That is, a fit of the low-temperature isotherms would predict a critical pressure, for example, that was too low by over a factor of 2. In short, the behavior of mercury is incompatible with the present equation of state.

VI. OTHER THERMODYNAMIC DATA

The equation of state is related by rigorous thermodynamic expressions to many other equilibrium properties, which can also be used as tests. In this section we give a selection of such tests, mostly for the mythical (12,6) fluid. These include the Helmholtz free energy, the internal energy, the vapor-pressure curve, the orthobaric liquid and vapor densities, and the Joule–Thomson inversion curve.

A. Helmholtz function

For T and ρ as independent variables, the fundamental thermodynamic function is the Helmholtz free energy $(U - TS)$ from which all other thermodynamic quantities are obtainable by differentiation. The excess Holmholtz free energy, relative to the ideal gas at the same temperature and

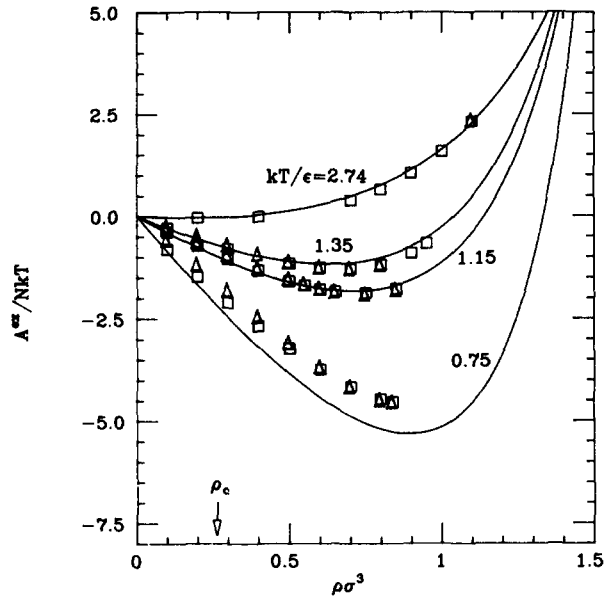

FIG. 15. The excess Helmholtz free energy as a function of density for a (12,6) fluid. The curves are from Eq. (33), the squares are computer simulations, and the triangles are results from the WCA theory.

density, is found from the equation of state by integration, leading to

$$\frac{A^{ex}}{NkT} = \int_0^\rho [B_2 - \alpha + \alpha g(d^+)]d\rho$$

$$= B_2\rho + \alpha\rho\left[\frac{b\rho(5-b\rho)}{(4-b\rho)^2}\right]. \quad (33)$$

Some values of A^{ex} for the (12,6) fluid are known from computer simulations[34] and from the WCA theory.[15,34] They are compared with Eq. (33) in Figs. 15 and 16.

The results at lower reduced temperatures appear in Fig. 15. The reduced critical temperature is about 1.35. Agreement with both the computer simulations and the WCA theory is good except at $kT/\epsilon = 0.75$. Here the WCA theory is better than the present results at high densities, but poorer at low. The discrepancies in A^{ex} at 0.75 do not have a large effect on the equation of state (see Fig. 6), which is related to the slope of the A^{ex} curve.

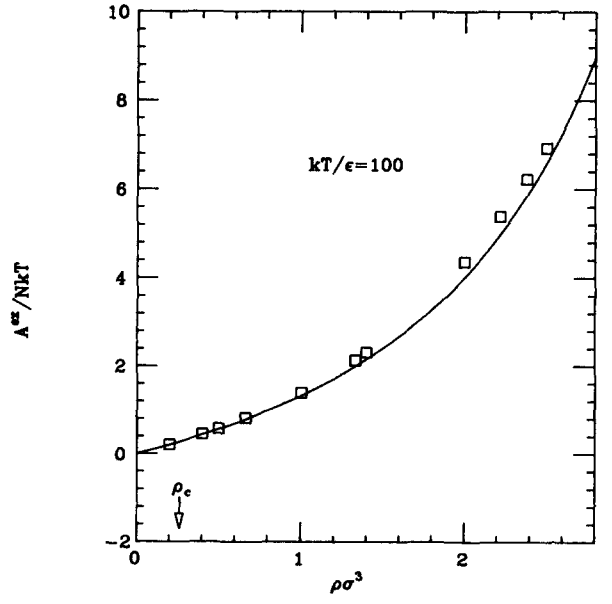

FIG. 16. Same as Fig. 15, for the highest available temperature.

The high-temperature results ($kT/\epsilon = 100$) are given in Fig. 16. The agreement with the computer simulations is good. No computer simulations of A^{ex} are available for reduced temperatures of 5 and 20. The WCA theory fails at high temperatures because its algorithm for calculating d breaks down.[34]

The present equation of state thus leads to a good representation of the fundamental thermodynamic equation for $A^{ex}(T,\rho)$.

B. Internal energy

The internal energy is of particular historical interest because one of the best-known results from the van der Waals theory is that the internal energy is linear in the density. For the present theory the excess internal energy, relative to the ideal gas at the same temperature and density, can be found by differentiation of Eq. (33) for A^{ex}:

$$\frac{U^{ex}}{NkT} = -\left(T\frac{dB_2}{dT}\right)\rho + (\alpha - b)b\rho^2\frac{(5-b\rho)}{(4-b\rho)^2}$$

$$-\left(T\frac{db}{dT}\right)\alpha\rho^2\frac{(20-3b\rho)}{(4-b\rho)^3}. \quad (34)$$

Only the first (linear) term is present for the van der Waals fluid, and it can be written in a universal form, the same for all temperatures, by means of the Boyle parameters,

$$\frac{U^{ex}(vdW)}{NkT_B} = -\frac{a}{kT_B}\rho = -v_B\rho. \quad (35)$$

A plot of U^{ex}/NkT_B vs $\rho\sigma^3$ is shown in Fig. 17 for the (12,6) fluid and for a van der Waals fluid matched at the Boyle temperature. Such a plot is *not* universal for the (12,6) fluid, but depends very noticeably on the temperature. Only the isotherms at or near the Boyle temperature, $kT_B/\epsilon = 3.418$, agree well with the van der Waals result, and then only at low densities. The agreement of Eq. (34) with the computer simulations[34] is fairly good. This is a more sensitive test of the equation of state than is A^{ex}, because the derivatives dB_2/dT and db/dT are involved.

The present equation of state thus also gives a good representation of the internal energy.

C. Vapor-pressure curve and orthobaric densities

The Maxwell construction on the p–v isotherms yields the following equation:

$$\frac{p_{sat}}{kT}\left(\frac{1}{\rho_g}-\frac{1}{\rho_l}\right) = \ln\left(\frac{\rho_l}{\rho_g}\right) + (B_2-\alpha)(\rho_l-\rho_g)$$

$$+ 8\frac{\alpha}{b}\left[\frac{6-b\rho_l}{(4-b\rho_l)^2} - \frac{6-b\rho_g}{(4b-\rho_g)^2}\right]. \quad (36)$$

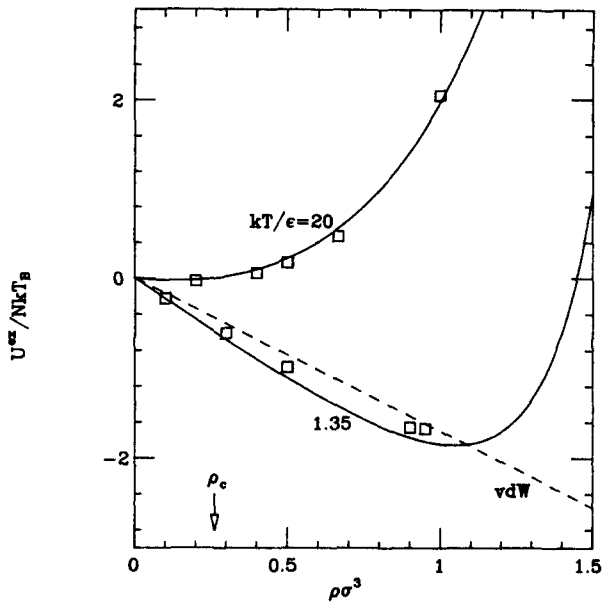

FIG. 17. Excess internal energy as a function of density for a (12,6) fluid and for a van der Waals fluid matched at the Boyle temperature (dashed line). The solid curves are from Eq. (34), and the points are computer simulations.

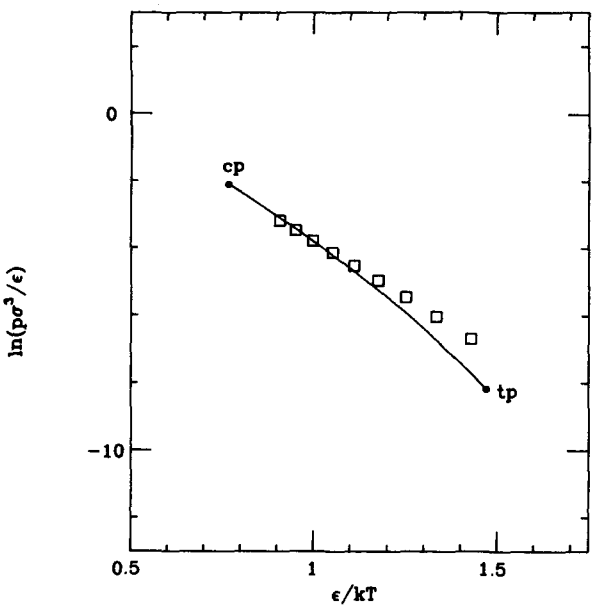

FIG. 18. Reduced vapor-pressure curve for a (12,6) fluid. The curve, terminated at the known critical and triple points, is calculated from the present equation of state, and the points are computer simulations.

Solved simultaneously with the equation of state itself, this yields the saturated vapor pressure p_{sat} and the orthobaric liquid and vapor densities, ρ_l and ρ_g. These quantities have also been calculated by Monte Carlo methods for the (12,6) fluid.[43]

The vapor-pressure curve as calculated from Eqs. (36) and (26) is compared with the computer simulations in Fig. 18, as $\ln p$ vs $1/T$ (in dimensionless units). The agreement is very good at the higher temperatures, but deviations are apparent as the triple point is approached. The calculated result is also more curved, implying a greater temperature dependence of the latent heat of vaporization.

The orthobaric densities calculated from Eqs. (36) and (26) are compared with the computer simulations in Fig. 19. The two lowest temperatures correspond to metastable liquid below the triple point. The vapor densities are reproduced very accurately, and the liquid densities fairly accurately. The calculated average density, the "rectilinear diameter," is linear near the critical point, as it should be for a classical mean-field theory, but shows a small curvature at lower temperatures.

On the whole, the boundaries of the two-phase region are fairly well reproduced by the present equation of state.

D. Joule–Thomson inversion curve

The Joule–Thomson inversion curve has been proposed as a very sensitive test of equations of state.[44] The Joule–Thomson coefficient is related to the equation of state by the thermodynamic formula

$$\mu_{JT} C_p = T\left(\frac{\partial V}{\partial T}\right)_p - V, \tag{37}$$

where C_p is the heat capacity at constant pressure. The inversion curve is determined by the condition $\mu_{JT} = 0$; for the present equation of state this yields

$$\left(T\frac{dB_2}{dT} - B_2\right) - b\left[1 - \frac{8(8-b\rho)}{(4-b\rho)^3}\right] + 2\alpha\left[1 - \frac{16(16-b\rho)}{(4-b\rho)^4}\right] + 16\alpha\rho\left(T\frac{db}{dT}\right)\frac{(10-b\rho)}{(4-b\rho)^4} = 0. \tag{38}$$

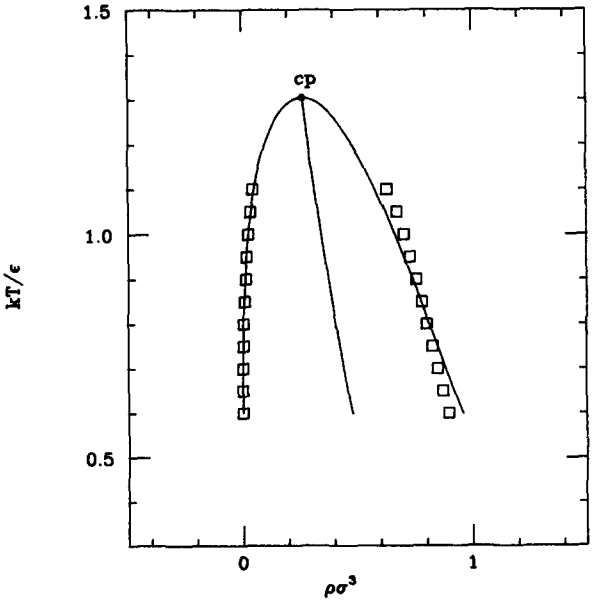

FIG. 19. Orthobaric liquid and vapor densities for a (12,6) fluid. The curve is calculated from the present equation of state, and the points are computer simulations. The calculated rectilinear diameter is slightly curved at the lower temperatures.

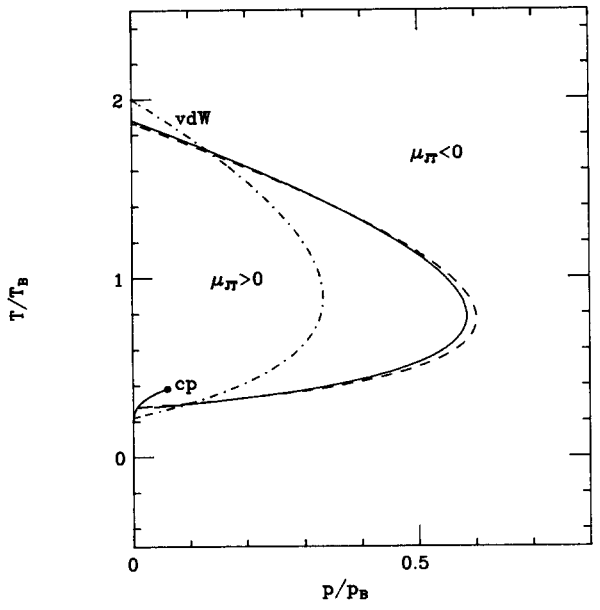

FIG. 20. Joule–Thomson inversion curves for the present and the van der Waals equations of state. The solid curve is based on the (12,6) potential and the dashed curve on the Aziz–Chen potential. The dot–dash curve is the van der Waals result. The lower branch of the inversion curve terminates on the vapor-pressure curve, which in turn terminates at the critical point.

Although no computer simulations for the inversion curve are available for the (12,6) fluid, there are several reasons why it is useful to calculate it from Eq. (38). First, it probes the equation of state at temperatures and pressures far above the critical. Second, it provides a different test of the sensitivity of the results to the potential model used to calculate α/v_B and b/v_B as functions of T/T_B. Finally, a comparison with the van der Waals result is of interest.

The results are shown in Fig. 20 in reduced units. The curves calculated for the (12,6) potential and the Aziz–Chen potential are very close. They would differ by more if the potential parameters ϵ and σ had been used for the reduction instead of the Boyle parameters T_B and p_B. Notice that most of the inversion curve extends far above the critical point. The van der Waals curve is quite different, especially the value of the maximum pressure.

The Joule–Thomson inversion curve thus seems to be reasonable, and insensitive to the model used to find α and b, provided that the Boyle parameters are used as reference values.

VII. DISCUSSION

We believe that the present equation of state, Eq. (26), comes close to solving the old van der Waals problem of an accurate analytical equation of state based on fundamental theory. The main new ingredients that make this possible are, first, the recognition that the structure of simple dense fluids is determined largely by the repulsive forces, and second, the availability of accurate simple approximations for $g(d^+)$. The application of suitable statistical-mechanical perturbation theory then leads to Eq. (26).

In the case of spherical molecules, for which the assumptions of the theory should apply most closely, the equation of state seems to work well up to quite high densities, including the liquid. This is about three times the critical density for noble gases and methane, and ten times the critical density for the (12,6) fluid. Even for the nonspherical molecule CO_2 the results are good up to about the critical density. Other thermodynamic properties related to the equation of state are also described well.

The results are less good near the critical point, as is not surprising for a mean-field theory. There are also some signs of inaccuracy near the triple point: See, for example, the high-density portion of the low-temperature curve for A^{ex} in Fig. 15, and the vapor-pressure curve of Fig. 18. Perhaps these latter deficiencies could be remedied by an improved algorithm for the effective van der Waals covolume b (equivalent to an effective hard-sphere diameter d), which is not directly supplied by the statistical-mechanical theory.

Although we have not considered them explicitly, nonspherical molecules and mixtures have an obvious place in the theory where they might be accommodated, namely in $g(d^+)$. This would of course involve the introduction of additional parameters. For mixtures, combination rules for unlike interactions would also be useful, but these are already available for pairwise interactions.[45,46]

A few further comments on the limitations of the theory are in order. It definitely is inapplicable to a substance like mercury, whose effective interaction potential varies significantly with temperature and density. Its applicability is also doubtful for substances like H_2O, and possibly NH_3, for which the attractive rather than the repulsive forces play a dominant role in the structure of the liquid.

Although the theory gives formulas for calculating the three temperature-dependent parameters of the equation of state from the intermolecular potential, it is only necessary to know the second virial coefficient as a function of temperature in order to use the equation in a predictive mode. The other two parameters, $\alpha(T)$ and $b(T)$, are insensitive to the shape of the potential, and all the results can be scaled with only two fixed parameters that can be found from the second virial coefficient. For this purpose we recommend not the potential parameters ϵ and σ, but the Boyle parameters defined by Eq. (28), whose use suppresses the peculiarities of any model used for the potential. We do *not* recommend using the critical parameters with any mean-field theory, since they may distort the rest of the equation of state. In this connection the following comment by Beattie and Stockmayer[29] is of interest:

"It was a cardinal point of the earlier workers that the equation of state constants be determined from critical data alone and not from the actual compressibility of a gas. As a result the compilations of van der Waals' constants found in various handbooks are utterly worthless for computing the volumetric behavior of gases."

ACKNOWLEDGMENTS

We thank Professor R. M. Stratt for many helpful discussions, comments, and suggestions, and Professor B. Caswell for several incisive questions and comments. The research was supported in part by NSF Grant No. 88-19370.

[1]J. D. van der Waals, *On the Continuity of the Gaseous and Liquid States*, edited with an Introductory Essay by J. S. Rowlinson, Studies in Statistical Mechanics Vol. 14 (North-Holland, Amsterdam, 1988).
[2]C. Dieterici, Ann. Phys. **69**, 685 (1899); **5**, 51 (1901).
[3]J. A. Beattie and O. C. Bridgeman, J. Am. Chem. Soc. **49**, 1665 (1927); **50**, 3133 (1928); Proc. Am. Acad. Arts Sci. **63**, 229 (1928).
[4]M. Benedict, G. B. Webb, and L. C. Rubin, J. Chem. Phys. **8**, 334 (1940).
[5]O. Redlich and J. N. S. Kwong, Chem. Rev. **44**, 233 (1949).
[6]J. J. Martin, Ind. Eng. Chem. **59** (No. 12), 34 (1967).
[7]A. Bejan, *Advanced Engineering Thermodynamics* (Wiley, New York, 1988), Chap. 6.
[8]M. Kac, G. E. Uhlenbeck, and P. C. Hemmer, J. Math. Phys. **4**, 216 (1963).
[9]G. E. Uhlenbeck, P. C. Hemmer, and M. Kac, J. Math. Phys. **4**, 229 (1963).
[10]P. C. Hemmer, M. Kac, and G. E. Uhlenbeck, J. Math. Phys. **5**, 60 (1964).
[11]P. C. Hemmer, J. Math. Phys. **5**, 75 (1964).
[12]L. Haar and S. H. Shenker, J. Chem. Phys. **55**, 4951 (1971).
[13]The history of this idea is discussed by Rowlinson in Ref. 1, Sec. 5.5.
[14]J. A. Barker and D. Henderson, J. Chem. Phys. **47**, 2856, 4714 (1967).
[15]J. D. Weeks, D. Chandler, and H. C. Andersen, J. Chem. Phys. **54**, 5237 (1971); **55**, 5422 (1971).
[16]Reviews are given by, among others, Rowlinson in Ref. 1 and by J. A. Barker and D. Henderson, Rev. Mod. Phys. **48**, 587 (1976).
[17]D. A. McQuarrie, *Statistical Mechanics* (Harper and Row, New York, 1976), p. 262.
[18]E. A. Mason and T. H. Spurling, *The Virial Equation of State* (Pergamon, Oxford, 1969), p. 13.
[19]L. Verlet, Phys. Rev. **165**, 201 (1968).
[20]P. Cutchis, H. van Beijeren, J. R. Dorfman, and E. A. Mason, Am. J. Phys. **45**, 970 (1977).
[21]N. F. Carnahan and K. E. Starling, J. Chem. Phys. **51**, 635 (1969).
[22]Y. Song, R. M. Stratt, and E. A. Mason, J. Chem. Phys. **88**, 1126 (1988).
[23]J. Tobochnik and P. M. Chapin, J. Chem. Phys. **88**, 5824 (1988).
[24]R. A. Aziz and H. H. Chen, J. Chem. Phys. **67**, 5719 (1977).
[25](a) L. Verlet, Phys. Rev. **159**, 98 (1967), as quoted by Barker and Henderson in Ref. 16; (b) C. K. Majumdar and I. Rama Rao, Phys. Rev. A **14**, 1542 (1976).
[26]N. B. Vargaftik, *Handbook of Physical Properties of Liquid and Gases*, 2nd ed. (English translation) (Hemisphere, New York, 1983).
[27]J. S. Rowlinson, Ref. 1.
[28]J. A. Beattie and W. H. Stockmayer, Rep. Prog. Phys. **7**, 195 (1940).
[29]J. A. Beattie and W. H. Stockmayer, in *Treatise on Physical Chemistry. Vol. 2. States of Matter*, 3rd ed., edited by H. S. Taylor and S. Glasstone (Van Nostrand, New York, 1951), Chap. 2.
[30]Reference 18, Sec. 2.9.
[31]These calculations are summarized in Ref. 18, Sec. 4.5.
[32]E. A. Guggenheim, Rev. Pure Appl. Chem. **3**, 1 (1953).
[33]A. E. Sherwood, A. G. DeRocco, and E. A. Mason, J. Chem. Phys. **44**, 2984 (1966).
[34]H. S. Kang, C. S. Lee, T. Ree, and F. H. Ree, J. Chem. Phys. **82**, 414 (1985).
[35]J. O. Hirschfelder, C. F. Curtiss, and R. B. Bird, *Molecular Theory of Gases and Liquids* (Wiley, New York, 2nd printing, 1964).
[36]F. Theeuwes and R. J. Bearman, J. Chem. Thermodyn. **2**, 171 (1970).
[37]A. Michels, T. Wassenaar, and P. Louwerse, Physica **20**, 99 (1954).
[38]L. F. Epstein and M. D. Powers, J. Phys. Chem. **57**, 336 (1953).
[39]B.-C. Xu and R. M. Stratt, J. Chem. Phys. **89**, 7388 (1988).
[40]R. H. Busey and W. F. Giauque, J. Am. Chem. Soc. **75**, 806 (1953).
[41]F. Hensel and E. U. Franck, Ber. Bunsenges. Phys. Chem. **70**, 1154 (1966).
[42]E. A. Moelwyn-Hughes, J. Phys. Chem. **55**, 1246 (1951).
[43]D. J. Adams, Mol. Phys. **32**, 647 (1976).
[44]D. G. Miller, Ind. Eng. Chem., Fundam. **9**, 585 (1970).
[45]K. T. Tang and J. P. Toennies, Z. Phys. D **1**, 91 (1986).
[46]J. Bzowski, E. A. Mason, and J. Kestin, Int. J. Thermophys. **9**, 131 (1988).